Natural convection with discontinuous wall-temperature variations

By JOSEPH A. SCHETZ
General Applied Science Laboratories, Inc., Westbury, New York

AND ROGER EICHHORN
Princeton University, Princeton, New Jersey

At present, solutions for natural convection problems involving discontinuous changes in wall temperature do not exist. This paper reports results of an extensive experimental investigation of the particular case of a vertical flat plate with a step-change in wall temperature. Temperature profiles and local heat transfer coefficients determined with a Mach–Zehnder Interferometer are presented for a wide range of the pertinent parameters. The flow field associated with this problem was studied by means of a series of Tellurium dye experiments in water. Photographs are presented showing representative flow patterns, and the stability of the flow is considered as a function of the ratio of the excess temperature below a discontinuity to the excess temperature above.

1. Introduction

The first successful study of laminar natural convection in the vicinity of a vertical flat plate was reported by Schmidt & Beckman (1930) who determined temperature profiles near a uniform temperature vertical plate by traversing the flow field with small diameter thermocouples. At the same time Pohlhausen (see Schmidt & Beckman 1930) presented an analysis based on a similarity transformation and obtained excellent agreement with the experimental results.

Sparrow (1955) and Sparrow & Gregg (1956, 1958) have presented analyses for restricted classes of wall-temperature variations by employing the Karman–Pohlhausen integral technique and by extending the similarity transformation method. Tribus (1958) has extended the integral analysis to include more general wall temperature variations. A recent experimental investigation (Hill 1961) has substantiated the analyses of Sparrow and Tribus for continuous, slowly varying wall-temperature distributions.

Many practical applications concern problems wherein the wall-temperature distribution is discontinuous. This particular type of non-similar boundary layer problem has, to date, successfully resisted attempts at analysis. The ordinary integral method is not applicable since the streamwise derivatives of wall temperature become singular at the location of the discontinuity. An approximate analysis based on a linearization of the convective derivative and collocation (Schetz 1961) failed to predict accurately the results of experiment despite the fact that the general technique gives good results for other non-similar boundary-layer problems including forced convection with discontinuous wall-temperature variations (Schetz 1963). The particular problem considered here is that of a vertical flat plate of length L (figure 1) whose temperature is constant at some value T_1 in the region $0 < x < x_0$ (x being a co-ordinate measured vertically upwards from the bottom of the plate) and is constant at some other value T_2 for $x_0 < x < L$. If T_1 and T_2 are both greater than the ambient temperature T_∞, the flow will always be upward and must, in the limit as $x \to \infty$, approach that associated with a plate heated uniformly to the value T_2. If on the other hand,

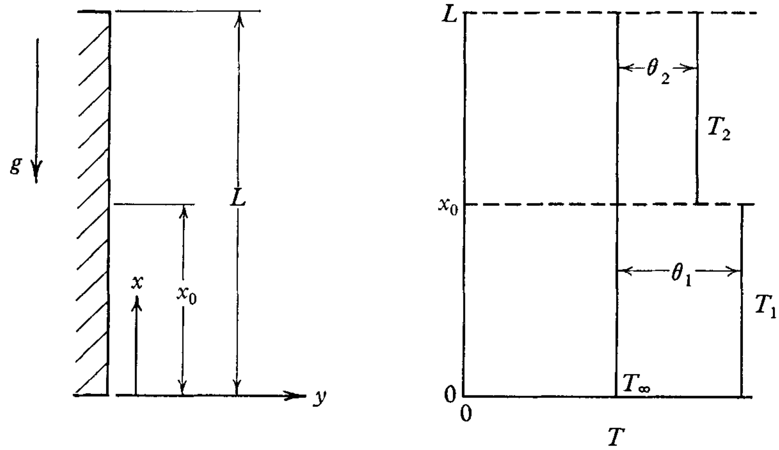

FIGURE 1. Co-ordinates used, and temperature distribution on the plate.

T_2 is less than ambient while T_1 remains greater than ambient, the flow develops from both the top and bottom leading edges of the plate. These opposing flows interact and separate from the plate surface. If the temperature excess on both the top and bottom portions of the plate are small so that the convective velocities are also small, the streams of fluid meet and issue from the plate as a pure laminar jet, which remains intact for some distance from the plate. As the temperature excess and thus the induced velocities become larger, the interaction of the two streams causes an essential instability in the flow field and the separation phenomena becomes unsteady in nature.

Lacking an adequate method of analysis, the results of an experimental investigation of this problem are reported here. Temperature profiles and heat-transfer distributions on a vertical flat plate with a single step change in wall temperature obtained with a Mach–Zehnder Interferometer are presented. All measurements were made in air (Prandtl number = 0·72) and the Grashof number based on the initial portion of the plate varied from 3×10^6 to 3×10^7.

As an auxillary study, a series of flow-visualization experiments was conducted using the Tellurium dye technique in water in the vicinity of a divided copper cylinder that could be heated at the bottom and cooled at the top. Photographs showing the flow pattern associated with the present problem are given and the basic stability of the flow is considered.

2. Description of apparatus

Interferometer

The advantages of studying fluid flow and convective heat transfer by optical means have long been appreciated and are well known. For natural convection problems, a Mach–Zehnder interferometer provides a direct measurement of the temperature variation throughout the flow field. Thus, for the purpose of performing the experimental work reported here and for the general development of capabilities for heat transfer research in the Mechanical Engineering Department at Princeton University, a sensitive Mach–Zehnder instrument was designed and constructed.

Photographs of the fringe patterns were taken with a Graflex 'Graphic View II' camera with a lens board modified to hold a 2 in. diameter Packard shutter. Some of the results were recorded on Polaroid Type 3000 film, others on Kodak Royal X-Pan.

Heat transfer model

The heat-transfer experiments were conducted using a fabricated copper plate, $16\frac{3}{4}$ in. wide and 20 in. high, supported within the test section of the interferometer. In order to provide for the desired step change character of the wall-temperature distribution, the plate was constructed of eight copper bars (figure 2)

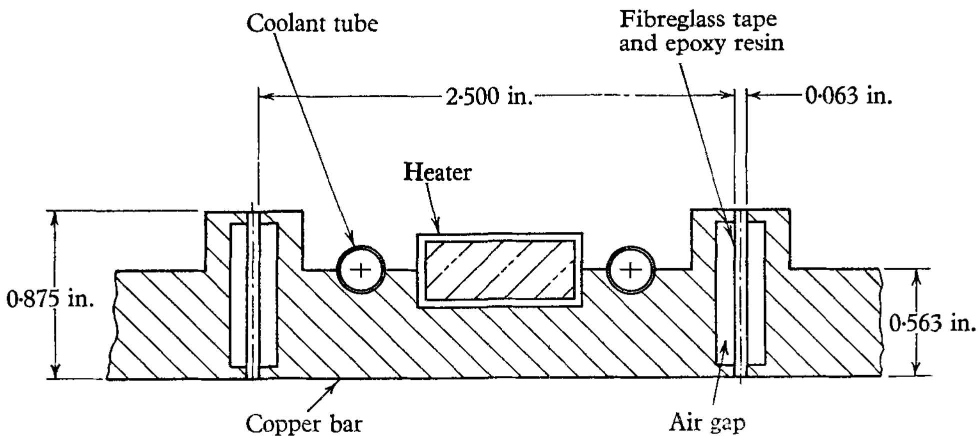

FIGURE 2. Heat transfer model detail; cross-section of typical segment.

which were joined side to side by a low conductivity junction consisting of fibreglass tape and epoxy resin. Each element can be heated by means of electric strip heaters or water cooled by two $\frac{1}{4}$ in. copper tubes soldered the full length of the bars. The heating is controlled by autotransformers and the coolant flow by needle valves mounted between the headers and coolant passages. The temperature of the coolant water is controlled by means of a refrigerator and a constant temperature bath.

The back of the model is covered with a $\frac{3}{16}$ in. Bakelite sheet and a $\frac{1}{4}$ in. steel plate to which a mounting bracket is attached. Wooden fairing pieces are fitted to the top and bottom edges of the model. Movable balsa wood shields are held to the sides of the model by four spring clamps. These shields help to keep the flow two-dimensional and reduce the flow of heat from the sides of the model. Each shield has a 2 in. by 2 in. opening arranged to hold a maple frame of the same size. A microfilm formed by pouring a small amount of commercial brushing lacquer on a still water surface (Bilgri 1960) is suspended across the frame forming a window.

The wall-temperature distribution was measured by means of 22 copper-constantan thermocouples mounted from the back of the model and insulated with copper oxide dental cement. All lead connexions were made within a large aluminium block to eliminate spurious e.m.f.'s resulting from temperature differences between connexions. An ice bath was used as a reference junction and the leads were taken through a Honeywell rotary switch to a Leeds and Northrup potentiometer.

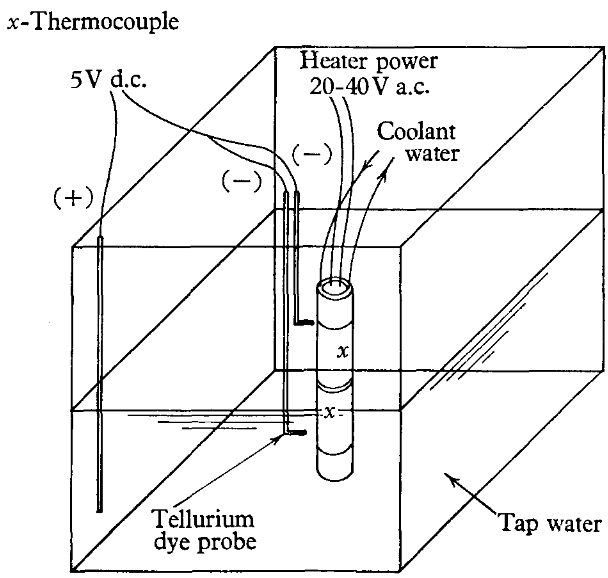

FIGURE 3. Tellurium dye flow visualization apparatus.

Flow visualization

Since interferograms of free convection flows relate to the temperature field alone, it was deemed highly desirable to obtain at least a qualitative picture of the flow field associated with free convection about vertical bodies having step changes in wall temperature.

The Tellurium dye technique developed by Wortmann (1953, 1955) and applied to free convection studies by Eichhorn (1961) was employed to study the flow in the vicinity of a divided copper cylinder electrically heated at the bottom and water-cooled at the top. The studies were conducted in tap water in a 5-gallon aquarium. The arrangement of apparatus is shown schematically in figure 3.

A Schlieren system was also arranged to permit continuous viewing of the flow since it was anticipated that some of the proposed wall-temperature variations might yield unsteady flows.

3. Results and discussion

Heat-transfer experiments

The interferometer adjustment employed for the determination of temperature profiles and local heat-transfer coefficients was such that a series of straight horizontal parallel fringes were produced on the screen for the unheated condition. When the temperature of the plate is raised above or lowered below the ambient temperature, the fringes shift on the screen and the temperature distribution can then be determined directly.

A list of the various cases investigated along with the boundary conditions employed for each is presented in table 1. In this table $\theta_1 = T_1 - T_\infty$, $\theta_2 = T_2 - T_\infty$ and Gr_{x_0, θ_1} is the usual Grashof number $g\beta\theta_1 x_0^3/\nu^2$, where β is the coefficient of thermal expansion and ν the kinematic viscosity of the fluid. In all cases but two (no. 2 and 8), the discontinuity in wall temperature was located at $x = 10$ in. Table 1 also lists the types of experimental results presented in this paper.

Case no.	T_∞ (°F)	θ_1 (°F)	θ_2 (°F)	θ_1/θ_2	x_0 (in.)	Gr_{x_0, θ_1}	Results†
1	75·7	24·8	31·0	0·80	10	$3{\cdot}03 \times 10^7$	*a, b*
2	76·3	25·2	—	1·00	—	3·08	*a, c*
3	75·6	24·6	22·4	1·10	10	3·01	*a*
4	75·0	25·6	21·0	1·22	10	3·12	*a, b, c*
5	74·7	25·1	12·6	1·99	10	3·06	*a, c*
6	74·3	24·7	5·1	4·85	10	3·02	*a*
7	75·3	24·7	0	∞	10	3·02	*a, b, c*
8	74·6	20·1	16·9	1·19	5	0·31	*a*

† *a*, Heat transfer; *b*, interferograms; *c*, temperature profiles.

TABLE 1. Experimental conditions.

Interferograms for three of the cases (no. 1, 4, 7) are shown in figures 4 to 6. In each case, the abrupt change in wall temperature at $x = 10$ in. is seen as a perturbation in the fringe pattern. The object masking a part of the undisturbed portion of the fringe pattern is a radiation-shielded thermocouple probe used to determine the ambient temperature, T_∞, and to provide a length scale on the photograph. Figure 4 represents an increasing step in wall temperature; figures 5 and 6 decreasing steps. Figure 6 is the interesting case (no. 7) where the upper surface ($x > x_0$) is cooled so that its temperature is equal to the ambient temperature.

Temperature profiles for cases 2, 4, 5 and 7 are shown in figures 7 to 10, respectively. The uniform wall temperature case (no. 2) was run to check the operation of the apparatus, and the resulting temperature profiles are compared with the theory of Ostrach (1953) in figure 7. The excellent agreement between theory and experiment on the basis of temperature profiles held for the heat-transfer coefficient as well. The temperature profiles in figures 8 to 10 clearly show the decay nature of the profiles after the step; the dotted curves shown represent the temperature profiles that would be obtained on a constant temperature plate.

Heat-transfer results for all the cases listed in table 1 are given in figure 11. The data is presented as q/q_{θ_1} *vs* x/x_0, where q_{θ_1} denotes the local heat-transfer

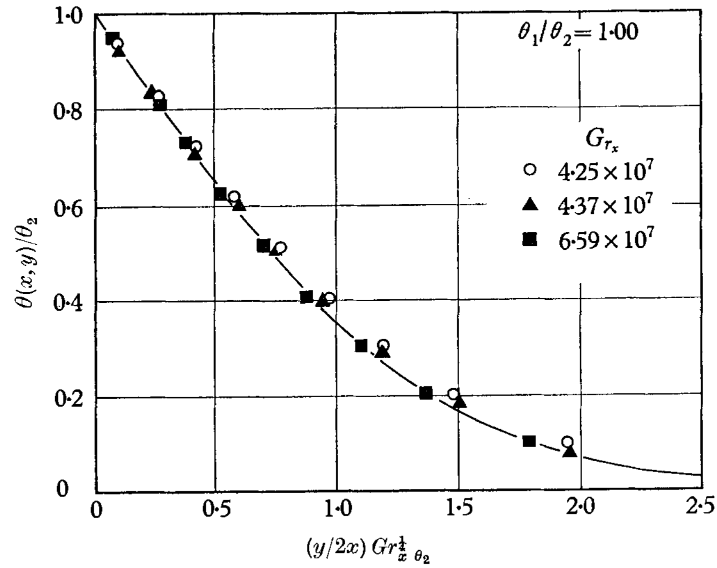

FIGURE 7. Temperature profiles for $\theta_1/\theta_2 = 1{\cdot}00$, $\theta_1 = 25$ °F. The solid line corresponds to the theory of Ostrach (1953).

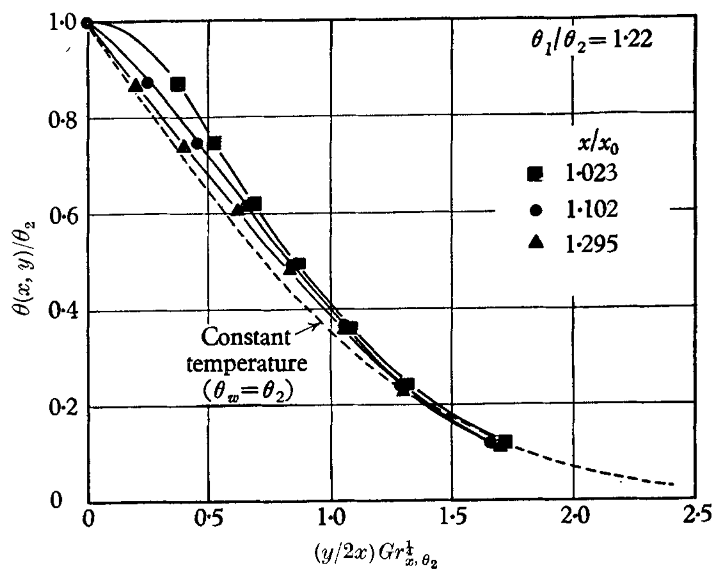

FIGURE 8. Temperature profiles for $\theta_1/\theta_2 = 1{\cdot}22$, $\theta_1 = 25$ °F.

rate that would be attained at the station of interest on a plate with a constant excess temperature, θ_1. From the analytical solution of Ostrach of the constant temperature (T_w) plate problem we have

$$Nu_x \equiv \frac{hx}{k} = 0{\cdot}401\, Gr^{\frac{1}{4}}_x, \tag{1}$$

where h is a Newtonian heat-transfer coefficient defined by the relation

$$q = h(T_w - T_\infty), \tag{2}$$

and k is the thermal conductivity of the fluid. Thus

$$q_{\theta_1} = 0\cdot401 \left(\frac{k\theta_1}{x}\right) Gr^{\frac{1}{4}}_{x,\theta_1}. \tag{3}$$

Now

$$q = -k \frac{\partial T}{\partial y}\bigg|_{y=0}, \tag{4}$$

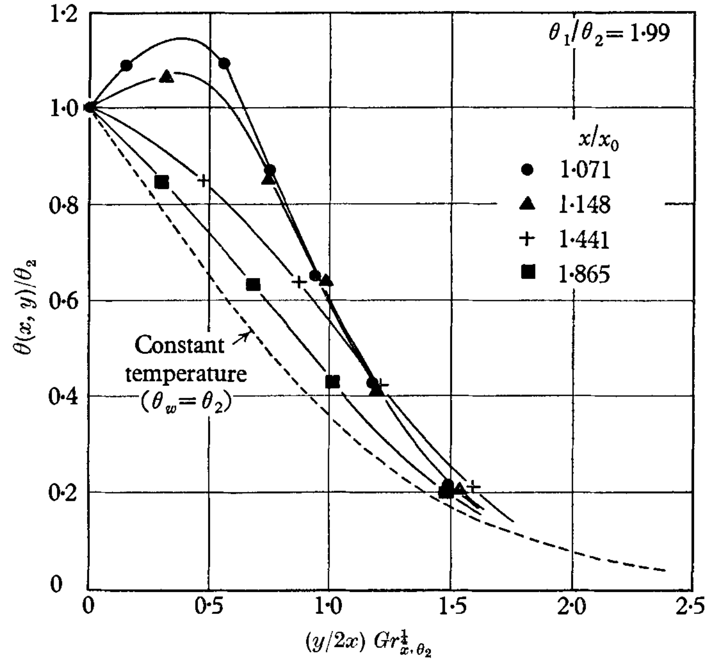

FIGURE 9. Temperature profiles for $\theta_1/\theta_2 = 1\cdot99$, $\theta_1 = 25\,°F$.

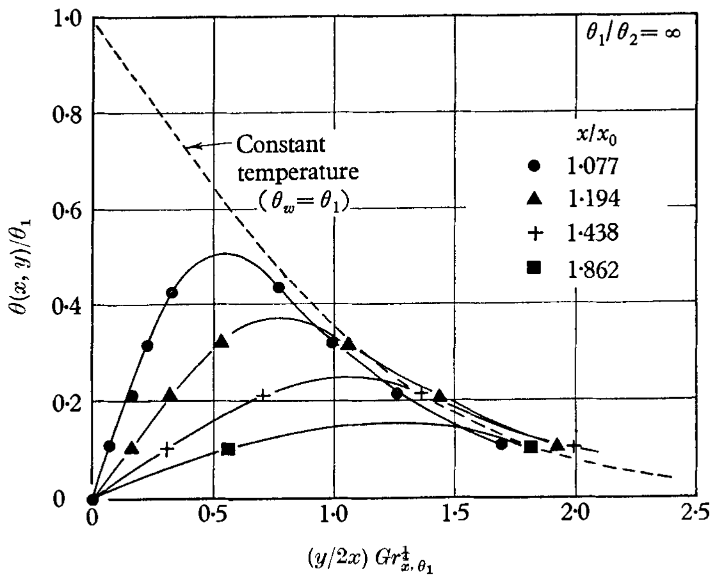

FIGURE 10. Temperature profiles for $\theta_1/\theta_2 = \infty$, $\theta_1 = 25\,°F$.

(y being the co-ordinate normal to the plate), and hence

$$\frac{q_2}{q_{\theta_1}} = -\left[2{\cdot}50\left(\frac{x_0}{\theta_1}\right) Gr_{x_0,\theta_1}^{-\frac{1}{4}}\right]\left(\frac{x}{x_0}\right)^{\frac{1}{4}}\frac{\partial T}{\partial y}\bigg|_{y=0}. \tag{5}$$

The slope of the temperature at the wall can be obtained by plotting temperature profiles or it can be related to the slope of the density of interference fringes ϵ at the wall, thus

$$\frac{\partial T}{\partial y}\bigg|_{y=0} = -\frac{T_w}{T_\infty}\frac{(T_w-T_\infty)}{\epsilon_\infty}\frac{\partial \epsilon}{\partial y}\bigg|_{y=0}. \tag{6}$$

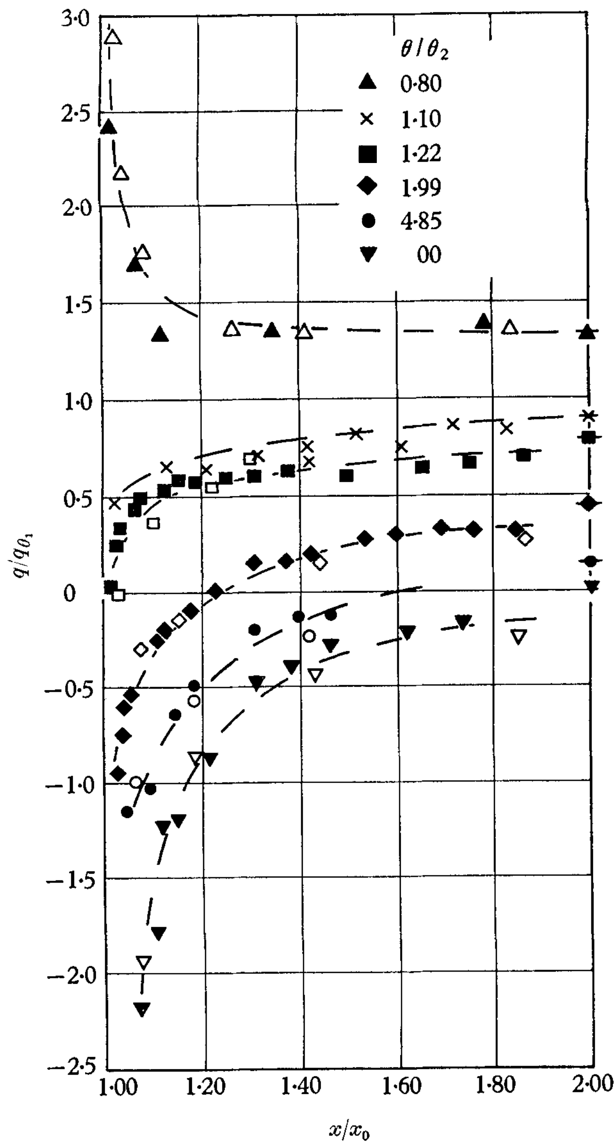

FIGURE 11. Local heat-transfer distributions.

Substituting (6) into (5), we have

$$\frac{q_2}{q_{\theta_1}} = \left[2{\cdot}50\left(\frac{x_0}{\epsilon_{\infty_2}}\right)\left(\frac{T_2}{T_\infty}\right)\left(\frac{\theta_2}{\theta_1}\right)Gr^{\frac{1}{4}}_{x_0,\theta_1}\right]\left(\frac{x}{x_0}\right)^{\frac{1}{4}}\frac{\partial \epsilon}{\partial y}\bigg|_{y=0}. \tag{7}$$

In figure 11 the open symbols represent points obtained by plotting temperature profiles and the solid symbols represent points obtained by measuring the slope of the fringes.

The finite plate used for these experiments can be considered as the beginning of an infinite plate at some temperature, T_2, having a starting length, x_0, at some temperature, T_1. As the distance from the step increases, the effect of the starting length diminishes until finally, at large distances, the local behaviour would be that associated with a constant temperature plate at T_2. This effect is manifested by $q/q_{\theta_1} \rightarrow (\theta_2/\theta_1)^{\frac{5}{4}}$ as $x/x_0 \rightarrow \infty$. This asymptotic value is indicated by a solid symbol at the extreme right-hand side of figure 11. The rapidity of the approach to the asymptote is, of course, strongly dependent upon $|\theta_1 - \theta_2|$ as can be readily observed from the plot.

Some experiments were conducted for negative values of θ_1/θ_2, i.e. the top portion of the plate was cooled and the bottom portion heated. As mentioned before, this results in opposing flows from the top and bottom leading edges of the plate. The results of the flow visualization studies reported below and recent smoke experiments performed at Princeton University by Mr Elliot Flicker using the flat-plate heat-transfer model described herein indicated that the flow field tends to be quite unsteady and three-dimensional in nature. Thus, data obtained with the interferometer assuming the flow to be two-dimensional must be viewed with considerable suspicion and only results for positive values of θ_1/θ_2 are given in this paper.

Finally, an experiment was conducted to investigate the effects of a Grashof number variation on the flow field. The distance to the step was decreased to 5 in. and the excess temperature on the bottom side was decreased to 20 °F to yield a Grashof number of 3×10^6 with $\theta_1/\theta_2 = 0{\cdot}80$. The results of this test agreed with that run at the higher Grashof number to an accuracy well within a reasonable experimental error.

Flow visualization

A systematic series of experiments was undertaken using the Tellurium dye flow visualization apparatus; the development of the flow field was investigated under a wide range of the parameters θ_1 and θ_1/θ_2. No fundamental difference in the character of the flow was observed as a result of a variation in θ_1 from 5 °F to 10, 15 and 20 °F, so only selected examples of the flow pictures obtained are presented.

Typical results are shown in figures 12 and 13 for $\theta_1/\theta_2 = -4$ and -2. The first value of θ_1/θ_2 indicates that the temperature excess on the top half of the cylinder is one-quarter of that on the bottom and that the wall temperature on the top is below ambient while that on the bottom is above. For such a case, the flow develops from the top and the bottom of the cylinder with the flow from below dominating. The flow in this case was quite steady and appeared stable. For

$\theta_1/\theta_2 = -2$, the flow from below still dominates but the stronger upper flow causes an inherent instability in the interaction region. The flow develops with a continuous undulating interface dividing the two flow regimes.

The general conclusions that can be drawn from this study are:

(i) The flow tends to be unsteady and is inherently so for $\theta_1/\theta_2 > -4$, (ii) there is little, if any, mixing of the upper and lower flow regions, and (iii) the interface is continuous and rippled in appearance.

REFERENCES

BILGRI, J. 1960 Indoor models—Part One. *Model Airplane News.*

EICHHORN, R. 1961 Flow visualization and velocity measurement in natural convection with the tellurium dye method. *Trans. ASME, Series C,* 379–81.

HILL, F. C. 1961 Free convection with non-uniform wall temperatures. Master's Thesis, Dept. of Mech. Engng, University of California, Los Angeles.

OSTRACH, S. 1953 An analysis of laminar free-convection flow and heat transfer about a flat plate parallel to the direction of the generating body force. *NACA Rep.* no. 1111.

SCHETZ, J. A. 1961 Natural convection in the vicinity of a vertical plate with a step-change in wall temperature, Ph.D. Thesis, Dept. of Mech. Engng, Princeton University.

SCHETZ, J. A. 1963 On the approximate solution of viscous flow problems. *J. Appl. Mech.* **30**, 263–68.

SCHMIDT, E. & BECKMANN, W. 1930 Das temperature and geschwindigkeitsfeld von einer warmeabgebenden senkrechten platte bei naturlicher konvecktion. *Tech. Mech. Thermodynamic,* **1**, 341–9 and 391–406.

SPARROW, E. M. 1955 Laminar free convection on a vertical plate with prescribed non-uniform wall heat flux or prescribed non-uniform wall temperature. *NACA TN* no. 3508.

SPARROW, E. M. & GREGG, J. L. 1956 Laminar free convection from a vertical plate with uniform surface heat flux. *Trans. ASME,* **78**, 435–40.

SPARROW, E. M. & GREGG, J. L. 1958 Similar solutions for free convection from a non-isothermal vertical plate. *Trans. ASME,* **80**, 379–86.

TRIBUS, M. 1958 Discussion on similar solutions for free convection from a non-isothermal vertical plate. *Trans. ASME,* **80**.

WORTMAN, F. X. 1953 Eine methode zur boebachtung unde messung von wasserstomugen mit tellur, *Z. angew. Phys.* **5**, 201.

WORTMAN, F. X. 1955 Untersuchung instaliler grenzschletschwingungen in einem wasserkanal mit der tellurmethode. 50 *Jahre Grenzschichtforschung.* Braunschweig: Vieweg.

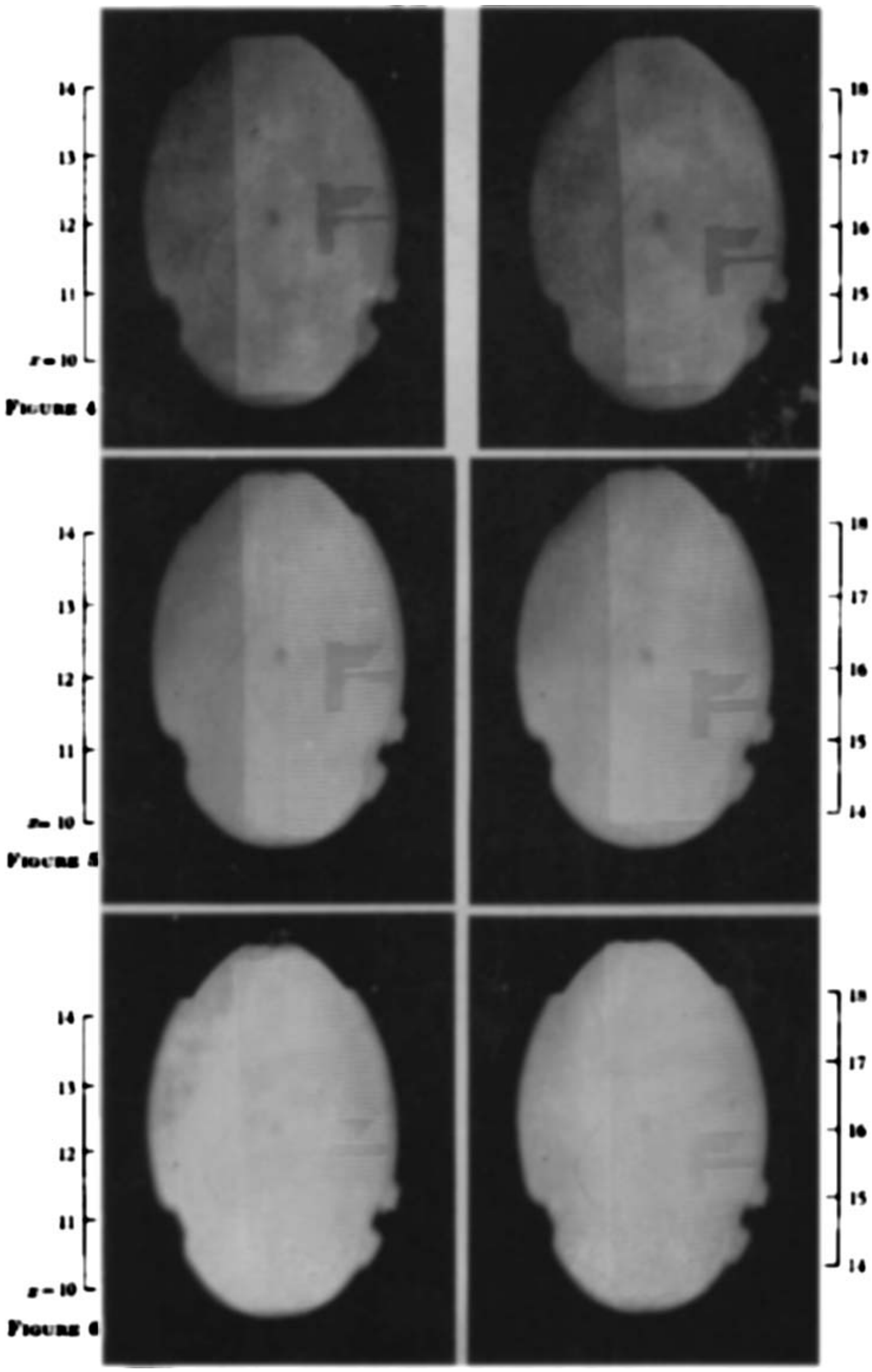

FIGURE 4. Interferogram $\theta_1 = 25$ °F, $\theta_1/\theta_2 = 0{\cdot}80$.
FIGURE 5. Interferogram $\theta_1 = 25$ °F, $\theta_1/\theta_2 = 1{\cdot}22$.
FIGURE 6. Interferogram $\theta_1 = 25$ °F, $\theta_1/\theta_2 = \infty$.

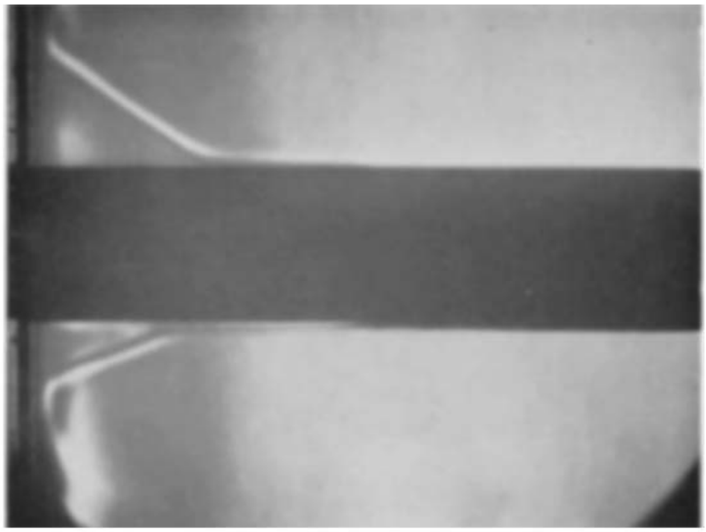

Schlieren photograph, $\theta_1/\theta_2 = -4$.

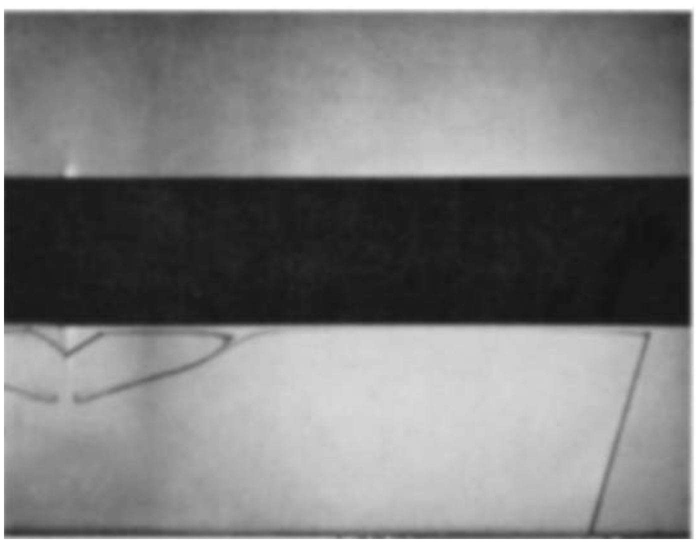

Tellurium trace, $\theta_1/\theta_2 = -4$.

FIGURE 12

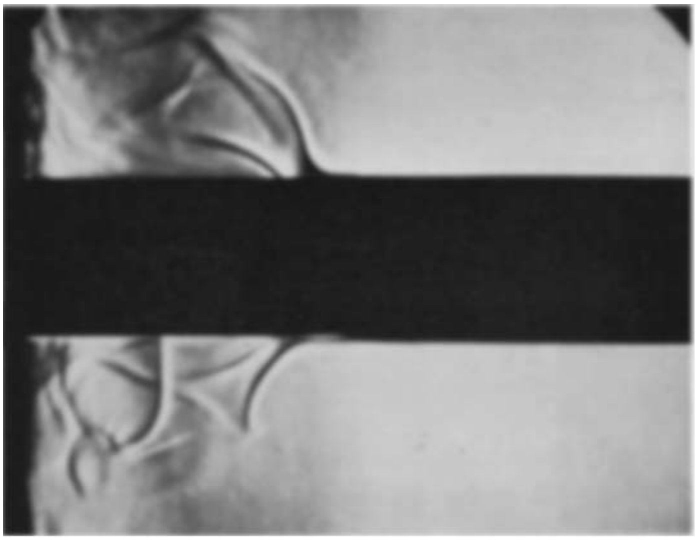

Schlieren photograph, $\theta_1/\theta_2 = -2$.

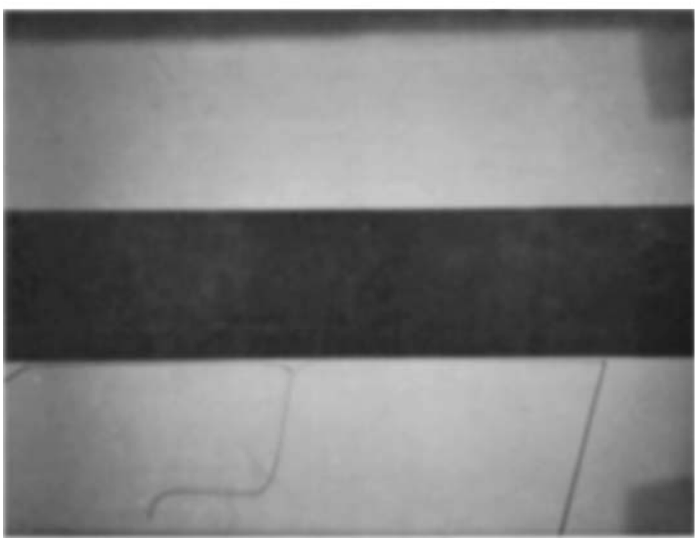

Tellurium trace, $\theta_1/\theta_2 = -2$.

FIGURE 13